

Enhancing Experimental and Numerical Data Validation through Acoustic Noise Signal Demodulation for Estimating Drone Propeller Rotational Speed

Gabriel Costa da Silva

Mateus Grassano Lattari

Federal University of Santa Catarina, UFSC

gabriel.silva@polo.ufsc.br

mateus.grassano@polo.ufsc.br

Lucas Bonomo Araújo

Julio Codioli

Racquel Knust Domingues

Augusto Barth Beck

Federal University of Santa Catarina, UFSC

lucas.bonomo@lva.ufsc.br

julio.codioli@ufsc.br

racquel.knust@lva.ufsc.br

augusto.barth.beck@gmail.com

Abstract. This study addresses a novel approach for estimating the rotational speed of small-scale propellers, typically found in drones, through the analysis of their acoustic noise signal. Accurately determining the instantaneous rotational speed of propellers in anechoic wind-tunnels poses significant challenges due to inherent experimental rotational speed fluctuations. These fluctuations can distort harmonic peaks levels, or deteriorate the process of applying comparable techniques when validating constant rotational speed numerical simulations with experimental data. This can be overcome by the knowledge of the propeller instantaneous rotational speed, allowing the signal to be resampled, correcting it to a constant rotational speed. Measured tachometer data is often not available nor reliable, as the use of external devices is not always feasible due to space constraints, costs, and sensitivity to adverse environmental conditions. An alternative approach is to directly estimate the propeller rotational speed from the measured acoustic signal, which is the focus of this study. The proposed methodology is based on the signal demodulation, which is a tachogless method that calculates the Hilbert Transform of the acoustic signal to obtain the frequency and phase related to the shaft rotation. To evaluate the technique, a synthetic propeller noise data are generated with a previous established rotational speed fluctuation, allowing a characteristic error for the algorithm predicted instantaneous rotation to be obtained. Secondly, the process is repeated for a real propeller noise signal, and the results are compared with the actual rotational speed measurement obtained with the tachometer. Finally, the obtained instantaneous rotation is employed to resample the experimental signal, allowing it to be suitable for validating numerical simulated signals. The spectra obtained from both signals are then compared, and the signal components are evaluated using a Time Synchronous Averaging (TSA) analysis. Preliminary results indicate the consistency and feasibility of the technique.

Keywords: Propeller noise, frequency estimation, signal processing, aerodynamic noise.

1. INTRODUCTION

In the ever-evolving realm of drone technology, the precise estimation of propeller rotational speed stands as a pivotal challenge. The need of knowing this information provides further analysis, such as dynamic control, precise noise sources identifications with decomposition techniques and failure prediction.

Upon scrutinizing the acoustic traits of noise produced by fully electric propulsion systems, it becomes apparent that the primary sources are the interactions between the blades and the airflow, encompassing turbulence and vortical effects. The dominant aspect of the noise spectrum comprises the tonal rendition, characterized by multiples of the blade-pass frequency (BPF), signifying a periodic signal. In contrast, the broadband feature, originating from the blade interactions, disperses energy throughout all frequency bands, exhibiting inherent stochasticity. In order to better analyze the noise sources, the features must be separated, which can express plenty difficulties, upon rotational speed fluctuations.

In this context, the Time Synchronous Averaging Method (TSA) (McFadden, 1987) finds extensive application in rotors operating at constant rotational speeds, owing to its straightforward implementation and effectiveness in isolating peaks. The method operates by averaging segments of acoustic data corresponding to a single rotation length in the time domain. However, its efficacy diminishes when applied to systems with varying speeds, as the irregular periodicity of

segments undermines its performance. Sharma and Parey (2016) proposed a tonal and broadband components TSA-based decomposition in order to calculate fault indicators in gears, which considers the rotational frequency fluctuation, therefore, this technique takes in account the tachometer signal, using n pulses per revolution. With this device it is possible to track the angular position of any shaft.

Small-scale propellers, typically found in drones, necessitate accurate measurement techniques amidst the backdrop of inherent experimental fluctuations. Traditional methods, reliant on tachometer data, often falter due to practical constraints and environmental sensitivities, prompting a quest for alternative methodologies. Peeters *et al.* (2019) presents a complete analysis on various methods that discard the need of a tacho signal.

Urbanek *et al.* (2011) investigate three major instantaneous frequency estimation techniques without any phase markers use in wind turbines speed tracking application. The spectrogram-based method proceeds with a maxima tracking due to the fact the peaks with the highest energy on the spectrogram should correspond to the value of the instantaneous frequency at each moment in time.

In another approach, Bonnardot *et al.* (2005) proposed a tacholess technique of estimating the instantaneous rotation of a shaft with limited frequency fluctuations. The method is based on the phase demodulation and utilizes the Hilbert Transform, a mathematical instrument to obtain the imaginary part of the analytic signal, which corresponds to the phase of the signal. The main achievement of this technique is that extincts the need of a tachometer, the instant rotation can calculated based on the shaft vibration data. This work analyses the merits and the feasibility of this method.

This work is organized as follows: Section 2 presents the methodology of the phase demodulation technique, describing in details the physics behind the numerical calculation. Section 3 describes some setups of both numerical and experimental data and Section 4 compares the results with the tachometer real information, as well as evaluates the components of the resampled signal with Time Synchronous Averaging (TSA) techniques. Finally, Section 5 concludes the consistency of the demodulation method.

2. METHODOLOGY

Section 1 introduces the importance of the study and begins with a literature review on the current advances in the field. This part of the study is aimed at presenting in details the methodology to be followed in order to perform the instantaneous frequency profile characterization of a propeller.

First, a widely used mathematical tool in the field of signal analysis is presented.

2.1 The Hilbert Transform

Consider a system with an input $x(t)$ and a filter $h(t) = \frac{1}{\pi t}$. The output of the system is given by:

$$y(t) = \hat{x}(t) = h(t) * x(t) = \frac{1}{\pi t} * x(t) \quad (1)$$

This convolution operation is called a Hilbert Transform (Shin and Hammond, 2008). Note that $h(t)$ is a non-causal filter with a singularity at $t = 0$. The Hilbert transform is often referred to as a 90° phase shifter. For example, the Hilbert transform of $\cos(\omega_0 t)$ is $\sin(\omega_0 t)$, and that of $\sin(\omega_0 t)$ is $-\cos(\omega_0 t)$.

The significance of the Hilbert transform is that it is used to form the so called "analytic signal" or "pre-envelope signal". An analytic signal is a complex time signal whose real part is the original signal $x(t)$ and where imaginary part is the Hilbert transform of $x(t)$, i.e. $\hat{x}(t)$. Thus, the analytic signal $a_x(t)$ is defined as:

$$a_x(t) = x(t) + i\hat{x}(t) = A_x(t)e^{i\phi_x(t)} \quad (2)$$

Where $A_x(t) = \sqrt{x^2(t) + \hat{x}^2(t)}$ is the instantaneous amplitude, and $\phi_x = \tan^{-1}(\hat{x}(t)/x(t))$ is the instantaneous phase.

2.2 The Demodulation Method

The primary method used for determining the instantaneous frequencies of a two-bladed propeller is the Demodulation Method (Bonnardot *et al.*, 2005), a robust and effective procedure that allows for a detailed and precise analysis of dynamic variations over time.

The technique consists of five main steps, each with its own peculiarities and conditions for optimal performance. This will be discussed in detail in Section 5, where the results will be presented.

Firtly, a characteristic harmonic of the signal is selected, with this study focusing on the first Blade Pass Frequency (BPF), which represents the harmonic with the highest energy. Subsequently, through a detailed visual analysis of the spectrum, a band-pass filter is applied to precisely isolate the region corresponding to the shaft rotation harmonic, along with its controlled frequency variations. This approach ensures a focused and accurate examination of the relevant dynamic behaviors. Fig. 1 demonstrated the frequency band selection for the filtering. It is important to add that the band of interest choice is primarily empirical, which results in testing band percentages and assess the performance of the ones

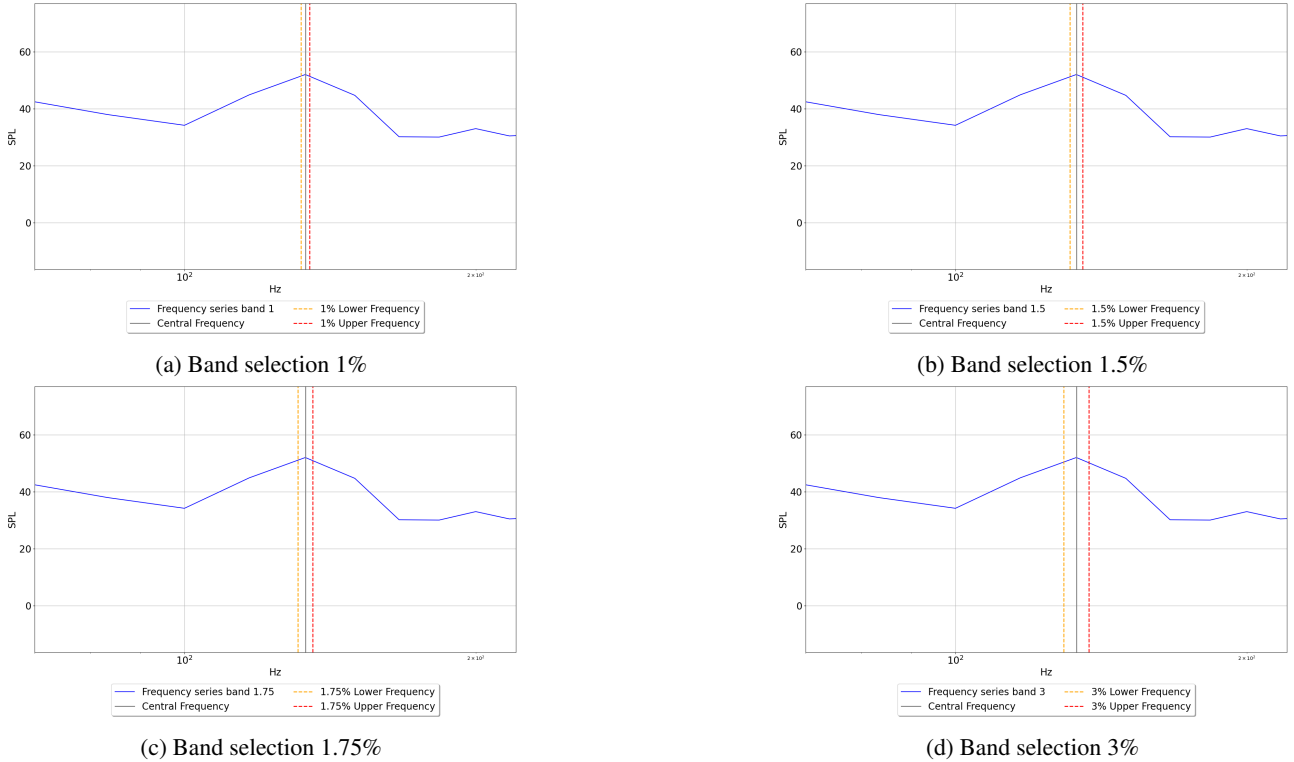


Figure 1: Band selection with different percentages.

who fit the problem the most. In this study we manage to compare multiple band percentages with the experimental instantaneous rotational frequency of the propeller.

Once the frequency band of the characteristic harmonic is selected, one may estimate the analytic signal according to 2, so that is possible to extract the analytical parameters of interest, such as the instantaneous phase of the propeller signal.

After the analytic signal is estimated, we shall extract the phase from one $\phi_x(t) = \tan^{-1}(\hat{x}(t)/x(t))$. The phase is then normalized by dividing the phase by the order m of the harmonic chosen in the first step.

$$\phi_{x,m}(t) = \frac{\phi_x(t)}{m} \quad (3)$$

After this normalization, the angular position of the propeller in radians is determined. In order to facilitate later mathematical manipulations, the phase is transformed into a first degree function to ensure the proportionality of the angular signal obtained. This can be done easily with a Numpy build-in function.

The phase markers are defined to identify the moment where the propeller completes one rotation, which is when the index corresponds to 2π radians. This is achieved through a linear interpolation between time and phase. From these markers, it is possible to establish a list that records the complete rotations, thus allowing the rotation period to be determined.

Finally, the speed profile can be traced based on the propeller rotation period, since:

$$f = \frac{1}{T} = \frac{1}{t_{i+1} - t_i} \quad (4)$$

Where the notation t_i is the time instant t where the phase marker i is generated.

3. Synthetic, numerical and experimental setups

In Sec. 2 was presented the demodulation techniques tested in this study to extract the instantaneous rotational frequencies of a propeller. The next step is to present the setups from which the data is created or extracted, so that is possible to test and check the feasibility of the method.

3.1 Synthetic Signal

Bonomo *et al.* tested some decomposition techniques aimed in experimental propeller data, where it took account the rotational speed fluctuations. In this work, the same formulation is used and it is shown in 3 steps (Bonomo *et al.*):

1. Generate a time array with the time-steps of $\Delta t \gg 1/fs$ where fs is the desired sampling frequency for the synthetic signal.
2. Generate a random instantaneous velocity array with the same length as the time array from step 1.
3. Re-sample the velocity array from step 2 to have the same fs as the desired synthetic signal. In this work, a cubic spline interpolation was used to provide a smooth curve. The resulting array is the instantaneous frequency, $f_i(t)$ to be used in:

$$\theta_i(t) = 2\pi \int_0^t f_i(t) dt \quad (5)$$

Finally, the synthetic signal is the sum of modulated harmonic signals, which can be given by:

$$p(t) = \sum_{n=1}^N A_n \sin(n\theta_i(t) + \phi_n) + w(t) \quad (6)$$

Where N is the number of harmonics, A_n is the harmonic amplitude, θ_i is the instantaneous phase angle defined in 5, ϕ_n is a random phase angle with a uniform distribution in the interval $[0, 2\pi]$ and $w(t)$ is a Gaussian white noise that represents the broadband component of the propeller signal.

3.2 Experimental setup

The UFSC Isolated Propeller Test Rig is installed in the semi-anechoic chamber at the Laboratory of Vibration and Acoustics (LVA/UFSC) (Beck *et al.*). The propeller rig structure primarily consists of an aluminum frame mounted on a steel column bolted to the ground. A brushless DC motor, specifically the U3 KV700 model from T-Motor, is utilized to drive motion to the propellers, in conjunction with an Electronic Speed Controller (ESC), the ALPHA 40A, also from T-Motor. Rotational speed and angular position monitoring are facilitated by a digital laser indexed encoder, the EM1 from US Digital, with 50 cycles per revolution (CPR). The rotational speed of the propeller is controlled via an in-house closed-loop PID controller, implemented in Python3, utilizing a PXIe-6368 Multi-function DAQ as a hardware interface. The controller operates with an average update rate of 30 Hz.

An array of microphones, oriented towards the ground, is positioned in line at a distance of 1.6 m from the steel column, parallel and 2 m away from the propeller axis. The array is arranged to cover a range from -45° to 45° , with 0° representing the rotor disk plane and positive angles measured above the rotation plane. Comprising nine GRAS 46AE 1/2" free-field microphones, the array includes positions at angular offsets of -27.5° , 0° and 27.5° , numbered 3, 5 and 7, respectively. The minimum ratio of the distance between microphones and the hub r to the propeller diameter d was $r/d = 6.5$, ensuring all microphones were positioned in the acoustic far field. The microphone array is presented in Fig.2.

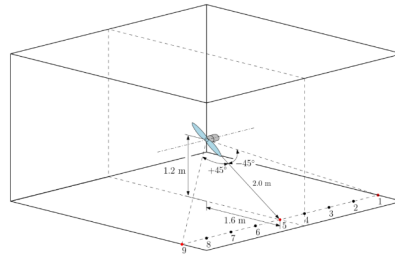


Figure 2: UFSC test rig microphone array displacement

All signals are simultaneously acquired using custom software implemented in Python3, utilizing the nidaqmx library. The signals are acquired with PXIe-4499 modules by National Instruments, with a sampling frequency of 51.2 kHz during 30 s runs for each test condition. (Beck *et al.*). The overview of the propeller mounted is shown in Fig.3.

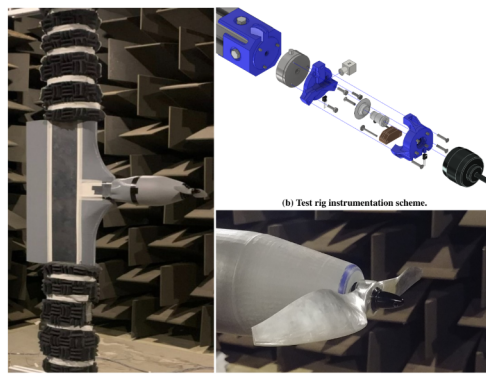


Figure 3: UFSC propeller test rig

4. Results

4.1 Synthetic signal

4.2 Experimental signal

Regarding the selection of the propeller signal frequency band, as mentioned in Section 2, the characteristic frequency of the harmonic given by the first BPF was chosen as the central frequency, characterized as the tone with the highest energy. The frequency band variation was 0.1%, 0.5%, 0.75%, 1%, 1.2%, 1.5%, 1.75%, 2%, and 3% of this frequency, both above and below.

In Fig. 4, 5 and 6 is shown the results given by analyzing different frequency bands from the experimental signal of the microphones 1, 5 and 9 of the experimental setup, which correspond to the hard right, hard left and the middle positions, respectively.

5. Conclusion

In Sec. 1 the current literature approaches for the problem stated. Sec. 2 presented the methodology of the selected technique to extract the instantaneous frequency of a shaft, but applied to a propeller signal, the called Demodulation method. In Sec. 3 is presented how the propeller data is gathered, whether is a synthetic or experimental signal, Sec. 4 shows the results from either of the two data types. In the current section, we provide the conclusion, the feasibility or accuracy of the method exposed.

After a visual inspection of the experimental results, it can be conclude that the band inspection is a primal parameter in order to obtain a great performance of the technique. For every microphone analysed, below 0.1%, it was observed that the instantaneous frequency variation was cut off due to the excessively narrow band in the spectrum, and above 3%, the result began to diverge due to the excessively wide band in the characteristic tone.

The better fitted band choices were the ones between 1% and 1.75% on every microphone position. Even though, for the hard right and left positions, the numerical results presented more aggressive peaks when compared with the middle microphone (5) as can be seen in Figures 4, 5 and 6, which can lead to larger error on the microphones more distant from the propeller.

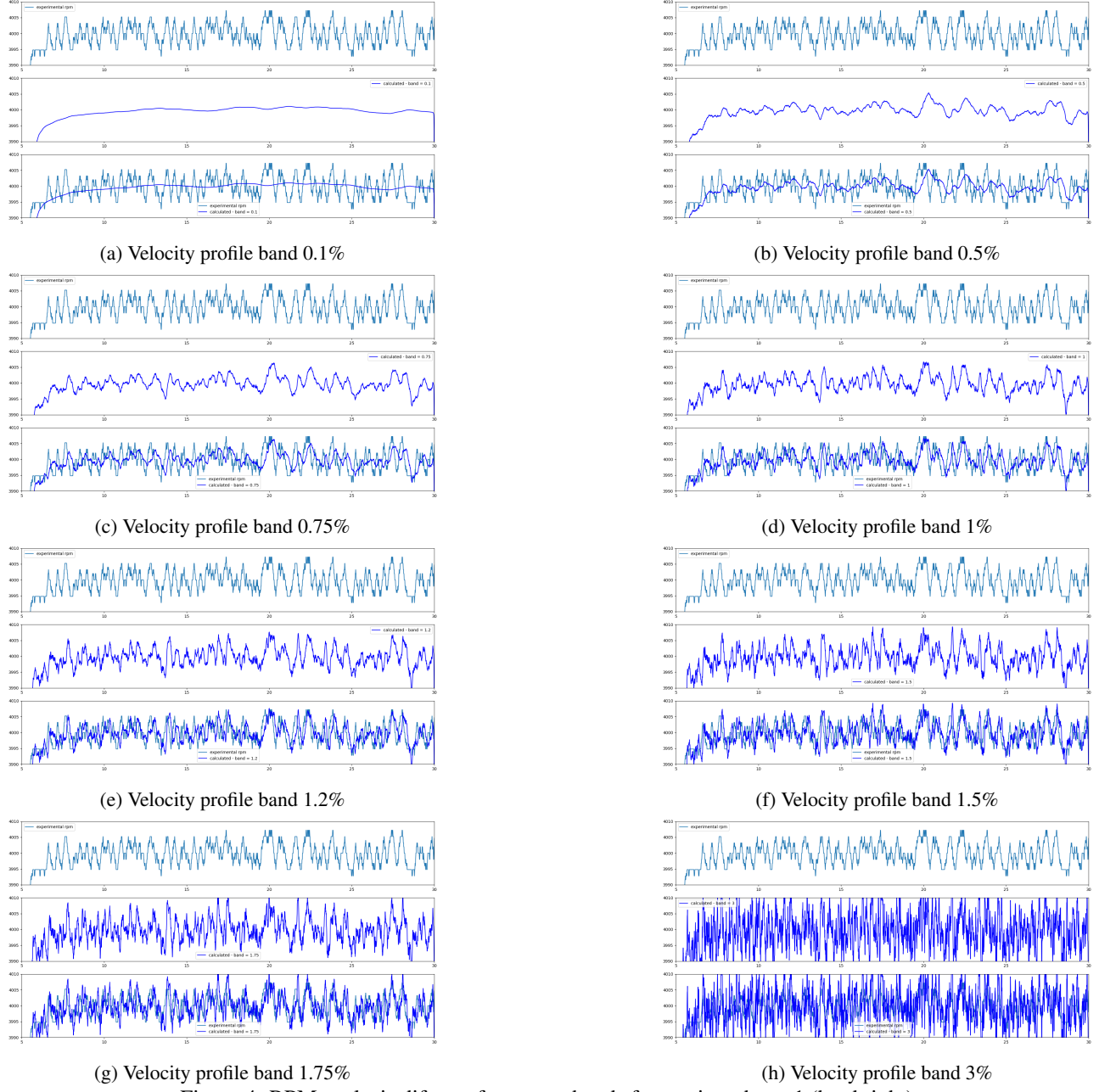


Figure 4: RPM analysis different frequency bands from microphone 1 (hard right).

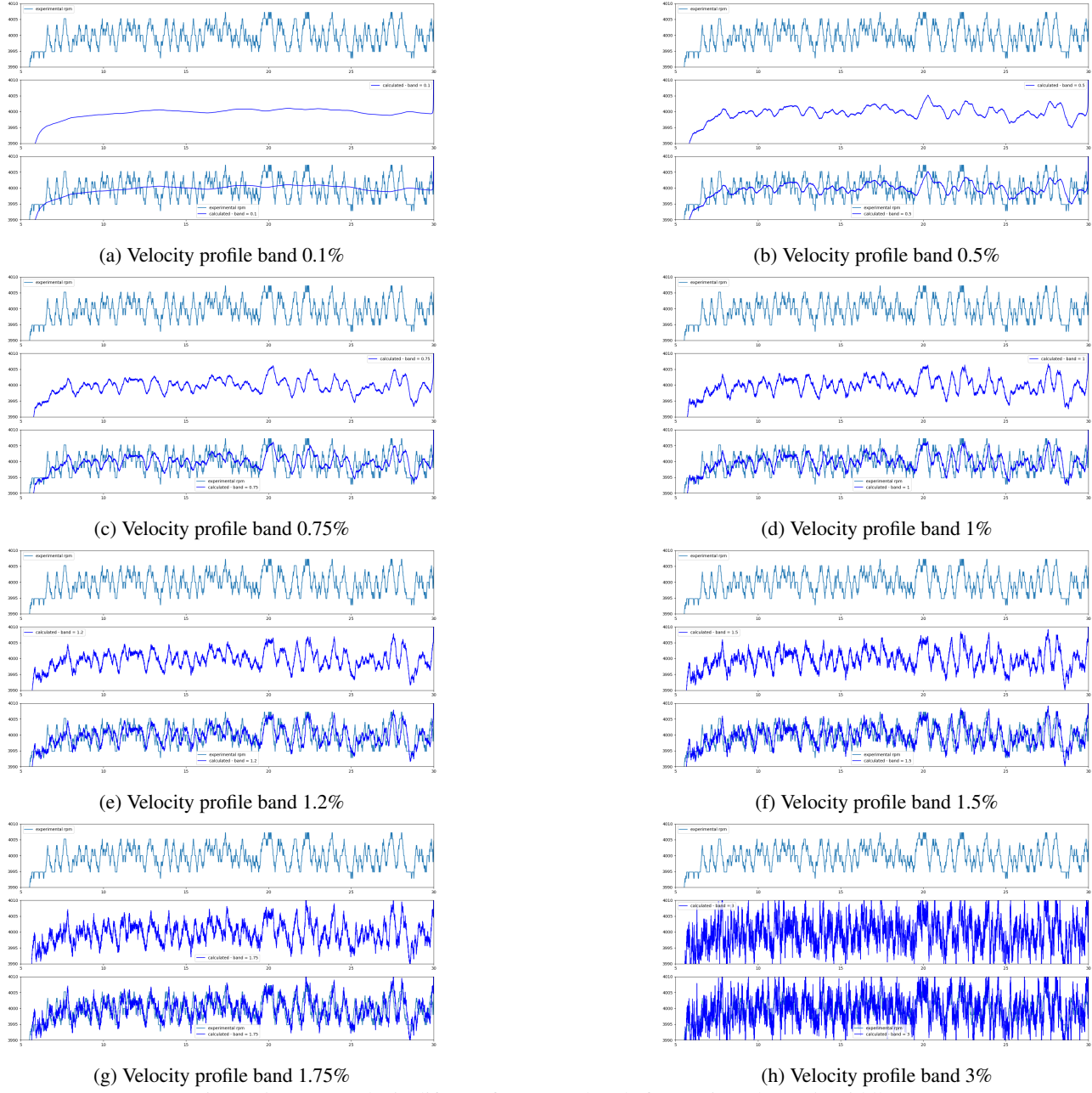


Figure 5: RPM analysis different frequency bands from microphone 5 (middle).

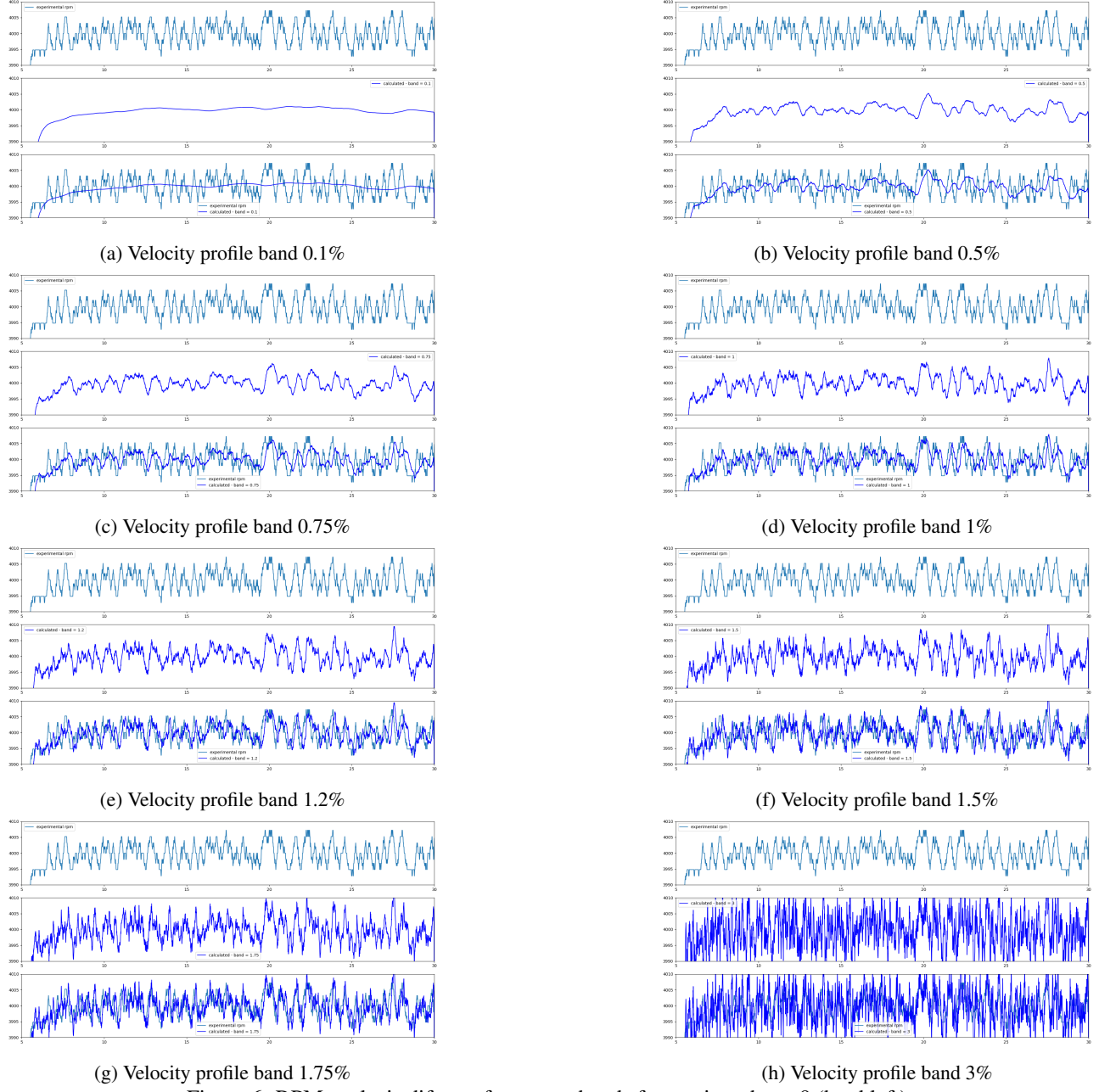


Figure 6: RPM analysis different frequency bands from microphone 9 (hard left).

- Beck, A.B., Cordioli, J.A., Bonomo, L.A., Fonseca, J.V.N., Simões, L.G., Tourinho, A.M., Casalino, D., Ragni, D. and Avallone, F., ???? *Comparative Assessment of Isolated Propeller Noise Test Rigs.* doi:10.2514/6.2024-3323. URL <https://arc.aiaa.org/doi/abs/10.2514/6.2024-3323>.
- Bonnardot, F., El Badaoui, M., Randall, R., Danière, J. and Guillet, F., 2005. “Use of the acceleration signal of a gearbox in order to perform angular resampling (with limited speed fluctuation)”. *Mechanical Systems and Signal Processing*, Vol. 19, No. 4, pp. 766–785. ISSN 0888-3270. doi:<https://doi.org/10.1016/j.ymssp.2004.05.001>. URL <https://www.sciencedirect.com/science/article/pii/S0888327004000664>.
- Bonomo, L.A., Cordioli, J.A., Colaciti, A.K., Fonseca, J.V.N. and Simões, L.G., ???? *Assessment of the Performance of Tonal-Broadband Decomposition Algorithms for Propeller Noise.* doi:10.2514/6.2023-3218. URL <https://arc.aiaa.org/doi/abs/10.2514/6.2023-3218>.
- McFadden, P., 1987. “Examination of a technique for the early detection of failure in gears by signal processing of the time domain average of the meshing vibration”. *Mechanical Systems and Signal Processing*, Vol. 1, No. 2, pp. 173–183. ISSN 0888-3270. doi:[https://doi.org/10.1016/0888-3270\(87\)90069-0](https://doi.org/10.1016/0888-3270(87)90069-0). URL <https://www.sciencedirect.com/science/article/pii/0888327087900690>.
- Peeters, C., Leclère, Q., Lindahl, P., Donnal, J., Leeb, S. and Helsen, J., 2019. “Review and comparison of tacholess instantaneous speed estimation methods on experimental vibration data”. *Mechanical Systems and Signal Processing*, Vol. 129, pp. 407–436. doi:10.1016/j.ymssp.2019.02.031.
- Sharma, V. and Parey, A., 2016. “Gear crack detection using modified tsa and proposed fault indicators for fluctuating speed conditions”. *Measurement*, Vol. 90, pp. 560–575. ISSN 0263-2241. doi:<https://doi.org/10.1016/j.measurement.2016.04.076>. URL <https://www.sciencedirect.com/science/article/pii/S0263224116301567>.
- Shin, K. and Hammond, J., 2008. *Fundamentals of signal processing for sound and vibration engineers*. Wiley. URL <https://eprints.soton.ac.uk/63688/>.
- Urbanek, J., Barszcz, T., Sawalhi, N. and Randall, R.B., 2011. “Comparison of amplitude-based and phase-based methods for speed tracking in application to wind turbines”. *Metrology and Measurement Systems*, Vol. 18, pp. 295–304. URL <https://api.semanticscholar.org/CorpusID:54750614>.

6. RESPONSIBILITY NOTICE

The following text, properly adapted to the number of authors, must be included in the last section of the paper:
The author(s) is (are) solely responsible for the printed material included in this paper.